Comparison of atmospheric mercury speciation and deposition at nine sites across central and eastern North America

Mark A. Engle,[1] Michael T. Tate,[2] David P. Krabbenhoft,[2] James J. Schauer,[3] Allan Kolker,[1] James B. Shanley,[4] and Michael H. Bothner[5]

Received 16 February 2010; revised 5 May 2010; accepted 10 May 2010; published 22 September 2010.

[1] This study presents >5 cumulative years of tropospheric mercury (Hg) speciation measurements, over the period of 2003–2009, for eight sites in the central and eastern United States and one site in coastal Puerto Rico. The purpose of this research was to identify local and regional processes that impact Hg speciation and deposition (wet + dry) across a large swath of North America. Sites sampled were selected to represent both a wide range of mercury exposure and environmental conditions. Seasonal mean concentrations of elemental Hg (1.27 ± 0.31 to 2.94 ± 1.57 ng m^{-3}; $\bar{x} \pm \sigma$), reactive gaseous mercury (RGM; 1.5 ± 1.6 to 63.3 ± 529 pg m^{-3}), and fine particulate Hg (1.2 ± 1.4 to 37.9 ± 492 pg m^{-3}) were greatest at sites impacted by Hg point sources. Diel bin plots of Hg^o and RGM suggest control by a variety of local/regional processes including impacts from Hg point sources and boundary layer/free tropospheric interactions as well as from larger-scale processes affecting Hg speciation (i.e., input of the global Hg pool, RGM formed from oxidation of Hg^o by photochemical compounds at coastal sites, and elemental Hg depletion during periods of dew formation). Comparison of wet Hg deposition (measured), RGM and fine particulate Hg dry deposition (calculated using a multiple resistance model), and anthropogenic point source emissions varied significantly between sites. Significant correlation between emission sources and dry deposition was observed but was highly dependant upon inclusion of data from two sites with exceptionally high deposition. Findings from this study highlight the importance of environmental setting on atmospheric Hg cycling and deposition rates.

Citation: Engle, M. A., M. T. Tate, D. P. Krabbenhoft, J. J. Schauer, A. Kolker, J. B. Shanley, and M. H. Bothner (2010), Comparison of atmospheric mercury speciation and deposition at nine sites across central and eastern North America, *J. Geophys. Res.*, *115*, D18306, doi:10.1029/2010JD014064.

1. Introduction

[2] Despite major advances in measurement of speciation and deposition of atmospheric mercury (Hg) over the last 20 years, significant challenges and knowledge gaps exist [*Mason et al.*, 2005; *Fitzgerald and Lamborg*, 2005]. In particular, the controls on Hg speciation and deposition are not well understood and appear to vary spatially [*Engle et al.*, 2008a; *Rutter et al.*, 2008; *Weiss-Penzias et al.*, 2009]. Due to the potential for atmospherically deposited Hg to be converted to toxic organic species, such as methyl mercury, factors determining Hg behavior have significant environmental consequences. For example, elemental Hg (Hg^o) is the dominant form of atmospheric Hg (~95%), exhibits a low solubility, and deposits rather slowly to the surface (0.02–0.15 cm s^{-1}) [*Seigneur et al.*, 2004]. By comparison, reactive gaseous mercury (RGM) and particulate Hg (Hg-P) species exhibit higher deposition rates and are thought to be more bioavailable, depending on their composition [*Lindberg et al.*, 2002; *Lyman et al.*, 2007; *Marsik et al.*, 2007].

[3] While several previous studies compared mercury speciation and deposition across a region, measurements have typically been limited to less than three sites spread across a relatively localized area [*Edgerton et al.*, 2006; *Lyman et al.*, 2007; *Engle et al.*, 2008a; *Rutter et al.*, 2008; *Weiss-Penzias et al.*, 2009]. In an attempt to identify processes that impact Hg speciation and deposition at a near-continental scale, this paper presents results from more than five cumulative years of data collected over the period of 2003–2009 at eight sites across the central and eastern United States and one site on the island of Puerto Rico. This research presents one of the largest data sets of atmospheric Hg speciation combined with wet + dry deposition.

[4] Due to expanding research highlighting the sensitivity of coastal areas to Hg inputs (see *Merritt and Amirbahman* [2009] for a review), this study focuses on differences in concentration, diel patterns, and deposition of atmospheric Hg at coastal sites relative to both rural and urban inland

[1]U.S. Geological Survey, Reston, Virginia, USA.
[2]U.S. Geological Survey, Middleton, Wisconsin, USA.
[3]Environmental Chemistry and Technology Program, University of Wisconsin-Madison, Madison, Wisconsin, USA.
[4]U.S. Geological Survey, Montpelier, Vermont, USA.
[5]U.S. Geological Survey, Woods Hole, Massachusetts, USA.

Copyright 2010 by the American Geophysical Union.
0148-0227/10/2010JD014064

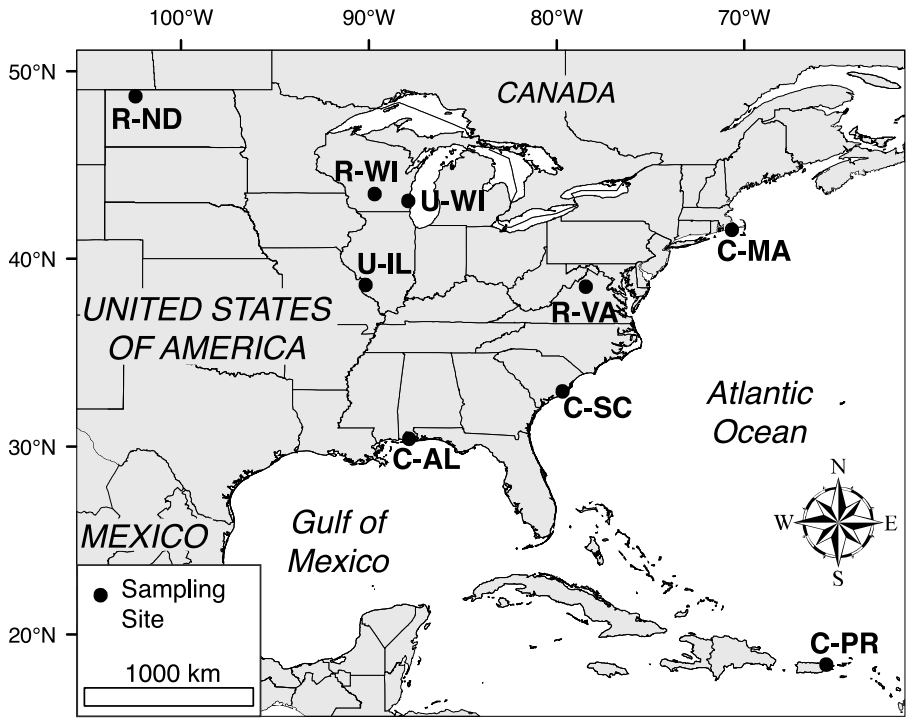

Figure 1. Map of locations of the nine sites investigated in this study.

sites. Previous workers have demonstrated that warm coastal sites exhibit peak concentrations of RGM that exceed values for rural inland sites (<15 pg m^{-3}) [*Valente et al.*, 2007] possibly as a result of Hg^o oxidation by photochemical species and input from Hg point sources in these coastal airsheds [*Malcolm et al.*, 2003; *Laurier and Mason*, 2007; *Engle et al.*, 2008a]. However, the geographic extent of these elevated RGM concentrations is not well constrained nor is the mechanism of coastal RGM production understood.

[5] To understand the controls on Hg^o and RGM concentration in different environments, seasonal average diel concentration plots were generated for the nine sites. Diel bin plots have previously been used to identify such processes as input from plumes, formation of RGM from Hg^o oxidation by photochemical compounds, dry deposition, emission of previously deposited Hg, meteorological mixing, boundary layer formation, and exchange with the free troposphere [*Obrist et al.*, 2008; *Stamenkovic et al.*, 2007, *Weiss-Penzias et al.*, 2009].

[6] In addition to comparing Hg speciation, the second objective of this research was to estimate wet Hg deposition and dry RGM and Hg-$PM_{2.5}$ deposition at the nine sites and to assess the impact of local and regional Hg sources on total deposition. Wet deposition is assessed simply by measuring the Hg concentration and volume of a precipitation sample collected at an individual site for a specified period of time, often as part of a regional study such as the Mercury Deposition Network (available at http://nadp.sws.uiuc.edu/MDN/). Because direct estimation of dry RGM and Hg-$PM_{2.5}$ deposition is potentially impacted with sampling and collection artifacts, the U.S. Geological Survey (USGS) and its collaborators developed a numerical resistance-based deposition model [*Tate et al.*, 2010]. This model is used in the present study to compare the magnitude of wet versus dry Hg deposition and the influence of total Hg emissions, which were taken from relevant U.S. and Canadian emissions inventories, on deposition rates.

2. Description of Sampling Sites

[7] For this paper, data sets were acquired from nine different sites investigated from 2003 to 2009 by the USGS and the University of Wisconsin-Madison. The sites include inland "rural" sampling areas with no significant Hg sources within a 25-km radius (R-WI, R-ND, R-VA), inland industrial sites, which are heavily impacted ("urban") by nearby Hg sources (U-WI, U-IL), and four "coastal" sites, which range from near pristine to moderately impacted by anthropogenic Hg sources (C-AL, C-SC, C-MA, C-PR; Figure 1). Table 1 provides additional information on the sampling periods, types of data collected, and magnitude of total Hg emissions at various distances from each of the sites. Additional location, elevation, meteorological, climate, and trace gas chemistry data for the sites are summarized in Table S1.[1]

[8] Data for the three rural sites were collected to assess impact of Hg transport from distal sources (>50 km) on otherwise background sites and, in the case of the R-WI site, to compare results with a nearby urban site (U-WI). Each rural site is characterized by total Hg emissions <20 kg/yr within a 50 km radius (Table 1) and is located in a relatively undeveloped area. The R-WI site is situated among a deciduous forest in Devil's Lake State Park in rural central Wisconsin. Previous interpretation of meteorology, air quality,

[1]Auxiliary materials are available in the HTML. doi:10.1029/2010JD014064.

Table 1. General Site Information, Duration of Hg Speciation Measurement, Source of Wet Deposition Data, and Magnitude of Hg Emission Sources

Site	Type	Start Date	End Date	Days of Data	MDN Wet Deposition Site[a]	Emission Sources at <10km (kg yr^{-1})	Emission Sources at 10–50km (kg yr^{-1})	Emission Sources at 50–125km (kg yr^{-1})	Data Source
R-WI	Rural Inland	10-Apr-03	19-Mar-04	344	WI31	0	18	816	*Rutter et al.* [2008], *Manolopoulos et al.* [2007a]
R-ND	Rural Inland	27-Apr-04	02-Jun-04	36	ND01	0	0	387	This Study
R-VA	Rural Inland	20-Jun-06	01-Sep-06	73	VA28	0	0	518	*Kolker et al.* [2008]
U-WI	Urban Inland	28-Jun-04	12-May-05	318	WI22	3.6	182	593	*Rutter et al.* [2008]
U-IL	Urban Inland	01-Dec-03	19-Feb-04	80	N/A	54	421	1208	*Manolopoulos et al.* [2007b]
C-AL	Coastal	13-Apr-05	29-Aug-05	138	USGS	0	15	821	*Engle et al.* [2008a]
		06-Jan-06	22-May-06	136					
C-SC	Coastal	23-May-06	22-May-07	364	SC05	0	330	399	This Study
C-MA	Coastal	01-Feb-08	06-Jan-09	338	USGS	0	6.4	107	This Study
C-PR	Coastal	28-Feb-06	09-May-06	70	USGS	0	1.4	199	Shanley et al., submitted manuscript (2010)

[a]Indicates which Mercury Deposition Network site the study site was co-located with (data available from http://nadp.sws.uiuc.edu/mdn/); those marked 'USGS' indicate wet deposition was collected and analyzed independently by the U.S. Geological Survey outside of the MDN network.

and Hg speciation data for the site by *Manolopoulos et al.* [2007a] and *Rutter et al.* [2008] concluded that 52% of reactive Hg (RHg; the sum of RGM and fine particulate Hg) and only 2% of Hg^o were derived from regional point sources while the remainder was contributed from non-point sources and the global Hg burden. The Lostwood National Wildlife Refuge (R-ND) site is located in a rural, hemiboreal region of North Dakota consisting of low, rolling hills covered by a grass prairie environment [*Sando et al.*, 2007]. The site was originally chosen for atmospheric Hg speciation in order to assess the potential impact from distal coal-fired power plants (Table 1). The third rural site is the hemiboreal Big Meadows site (R-VA) in Shenandoah National Park, Virginia. The R-VA site is located at an elevation of 1,100 m, approximately 800 m above the valley floor, in a large break among a deciduous forest along the crest of the Blue Ridge Mountains. *Kolker et al.* [2008] found that Hg^o and RGM concentrations at that site were typical of background sites except for a few afternoon RGM peaks (>30 pg m^{-3}), which corresponded to periods of elevated SO_2 and were attributed to distal anthropogenic Hg emissions. The R-VA site is unique in that it is typically situated within the free troposphere except during the afternoon, when convection and mixing increase the height of the boundary layer to above the elevation of the site [*Poulida et al.*, 1991].

[9] To focus on inputs from significant local and regional Hg emission sources, data from two heavily impacted urban sites were also examined. Elemental Hg and RHg concentrations measured in Hg-plumes at the heavily industrial U-IL site in East St. Louis, Illinois (metro. Pop. ~2,800,000), exceeded concentrations found at background sites by orders of magnitude (Hg^o up to 235 ng m^{-3} and RHg up to 5000–38,300 pg m^{-3}) [*Manolopoulos et al.*, 2007b]. *Manolopoulos et al.* [2007b] suggested that the large magnitude of the RHg concentrations and the similarity of ratios of SO_2:Hg in plumes to those reported for point sources indicated that local anthropogenic sources were the primary source of elevated Hg concentrations at the site.

[10] The second inland urban site (U-WI) is in downtown Milwaukee, Wisconsin, an urban area with a metropolitan population of ~1,700,000. *Rutter et al.* [2008] compared Hg^o and RHg time series concentration data between the U-WI and R-WI sites and found that concentrations of the two species were on average 56% and 83% greater, respectively, at U-WI than R-WI and that the U-WI measurements were heavily impacted by local and regional anthropogenic Hg sources.

[11] Data from four coastal sites adjacent to the Atlantic Ocean were included to contrast with the five rural and urban inland sites. The coastal sites varied substantially in latitude from 18° 20′ N (C-PR) to 41° 32′ N (C-MA), seasonal average temperature (see Table S1), climate, and magnitude of local and regional total Hg emission sources (Table 1). The subtropical coastal site near Weeks Bay, Alabama (C-AL), is situated near a rural backwater embayment along the central U.S. Gulf Coast. The area around the site contains several coal-fired power plants and the nearby city of Mobile (metro. Pop. ~400,000), but few Hg sources are located within 50 km of the site (Table 1). Results for the site, described by *Engle et al.* [2008a], include elevated RGM concentrations (up to 92.7 pg m^{-3}), which followed a strong diel pattern of

low RGM in the early morning, increasing in the morning to a mid-day maximum, and then decreasing at night. Elevated RGM concentrations in the afternoon were primarily attributed to oxidation of Hg^o to RGM by photochemical compounds.

[12] The second coastal site (C-SC) is located in an opening of humid subtropical mixed forest along the coast ~25 km northeast of Charleston, South Carolina (metro. Pop. ~600,000). Although contained within the Cape Romain National Wildlife Refuge, the area is surrounded by a variety of anthropogenic Hg sources including coal-fired power plants, pulp/paper production facilities, and metal processing plants (Table 1).

[13] The third coastal site (C-MA), located on the southwestern tip of Cape Cod, Massachusetts, features much colder conditions than the other coastal sites (see Table S1). The site, on the Quissett campus of Woods Hole Oceanographic Institution, is located roughly 65 km E of Providence, Rhode Island (metro. Pop. ~1,600,000), and 95 km SE of Boston, Massachusetts (metro. Pop. ~4,500,000). Few Hg sources are located within 50 km of the site (Table 1).

[14] The final coastal site investigated in this study is located in the tropical Luquillo National Forest of northeastern Puerto Rico (C-PR). There are no significant Hg sources or cities upwind of the site, which is generally considered to be pristine (Table 1). Mercury speciation results from C-PR demonstrate that despite extremely high wet deposition rates, concentrations of Hg^o and RGM are at background levels and predominantly controlled by the global Hg pool (J. B. Shanley et al., High mercury wet deposition at a "clean air" site in Puerto Rico, submitted to *Environmental Science and Technology*, 2010).

3. Methods

3.1. Mercury Speciation Measurement and Data Quality

[15] A Tekran 2537A cold vapor atomic fluorescence spectrometer (CVAFS) with 1130 and 1135 speciation attachments was used to collect and measure Hg^o, RGM, and Hg-$PM_{2.5}$ in near real-time. All data presented in this paper were collected by a small group of USGS and University of Wisconsin-Madison personnel who used similar operational and QA/QC methods. For data collected at the R-WI, R-VA, U-WI, U-IL, C-AL, and C-PR sites, sampling and analysis methods are described in previous publications [*Manolopoulos et al.*, 2007b; *Kolker et al.*, 2008; *Engle et al.*, 2008a; *Rutter et al.*, 2008; Shanley et al., submitted manuscript, 2010]. For the remaining sites, Hg speciation data were collected using standard USGS methods and QA/QC as described by *Engle et al.* [2008a]. For all sites, inlets of the Hg speciation units were placed at heights of 4–8 m above ground surface. Briefly, the unit operates on a 2-h schedule; the first hour is dedicated to collection of RGM on a KCl-coated annular denuder, impaction of Hg-$PM_{2.5}$ onto a regenerating particulate filter, and measurement of Hg^o concentration in twelve consecutive 5-min averages. During the second hour of the cycle, the system is purged with Hg-free air, and the collected Hg-$PM_{2.5}$ and RGM are consecutively analyzed after pyrolysis and conversion to Hg^o. All Hg^o, either collected directly from the atmosphere or generated from pyrolysis of the denuder or particulate filter, is collected on one of two gold traps. The traps operate sequentially in 5-min cycles in which one trap is heated and analyzed via CVAFS while the other trap collects Hg^o in the sampling line. Every two hours the setup provides twelve consecutive 5-min average Hg^o concentration measurements and 1-h average RGM and Hg-$PM_{2.5}$ concentration measurements. The CVAFS was calibrated every 1–7 days with an internal permeation source, which was checked against manual Hg^o injections every 1–2 months. Annular denuders were replaced every 2–4 weeks and the regenerating particulate filter every 1–2 months. Bias checks between the two gold traps showed average differences of < 5%. Data for which trap bias was > 10% were discarded from further analysis. Data coverage of Hg^o at the sites during the periods of study ranged from 47 to 94% with a mean of 71%; RGM and Hg-$PM_{2.5}$ both ranged from ~25–90% with a mean of ~70%.

[16] To ensure that differences in concentrations of Hg species between sites are a result of environmental variability rather than analytical differences between instruments, intercomparison tests were conducted on multiple Tekran Hg speciation units. The units were attached to a high-volume, unheated manifold for two periods in April 2007 (n = 4 units) and November 2008 (n = 3 units) for a total of more than 19 days of operation. The speciation units were exposed to ambient air, Hg^o-spiked ambient air, and RGM-spiked ambient air. Percent relative standard deviation (%RSD) among the instruments for the April 2007 and November 2008 events were 5.9% ($\bar{x}$ Hg^o = 10.9 ng m^{-3}) and 4.5% ($\bar{x}$ Hg^o = 4.37 ng m^{-3}) for Hg^o, 34.2% ($\bar{x}$ RGM = 2.6 pg m^{-3}) and 11.4% ($\bar{x}$ RGM = 16.1 pg m^{-3}) for RGM, and 8.3% ($\bar{x}$ Hg-$PM_{2.5}$ = 5.8 pg m^{-3}) and 38.2% ($\bar{x}$ Hg-$PM_{2.5}$ = 14.1 pg m^{-3}) for Hg-$PM_{2.5}$, respectively. For RGM and Hg-$PM_{2.5}$, %RSD generally decreased when concentrations exceeded 15 pg m^{-3}. To assess the precision and accuracy of RGM measurement by the Hg speciation units, 28 pre-spiked denuders (Frontier Geosciences), each bearing 48.4 pg of $HgCl_2$ (an RGM surrogate), were analyzed by three of the speciation units. The high recovery rate (98.6 ± 13.1%) of $HgCl_2$ from the denuders indicates that the multiple units precisely and accurately measure RGM concentrations. Results from these intercomparison tests provide bounds on analytical uncertainty due to instrument differences for the data presented in this paper.

[17] A high proportion of RGM and Hg-$PM_{2.5}$ concentration data (often > 40%) were below instrument detection limits and were reported as zeros. To avoid errors in statistical calculations as a result of arbitrarily assigning a zero value for these data points, all summary statistics and statistical testing were estimated using Kaplan-Meier methods for data sets containing nondetects [*Helsel*, 2005]. Statistical analyses were performed using R version 2.10 and NCSS 2007.

3.2. Creation of Bin Plots

[18] To identify diel patterns of Hg^o and RGM concentrations at the various sites, diel bin plots were created for each species and season. The plots show mean ± standard deviation ($\bar{x} \pm \sigma$) for each 2-h period (starting with 12:01 A.M.–2:00 A.M.) of each season. To minimize overlap of the data in the plots, standard deviation values were divided by four. Diel bin plots have previously been used

Table 2. Percent Land Cover for a 10-km Radius Around Each Site Based on the U.S. National Land Cover Database[a]

Land Use Category[b]	Land Cover[c]	R-WI[d]	R-ND	R-VA	U-IL	U-WI	C-AL	C-SC	C-MA	C-PR
Water	Open Water	5.0	**4.7**	0.0	**7.6**	**51.2**	**21.9**	**29.1**	**67.9**	**85.8**
Urban	Developed (Any Intensity)	9.7	3.3	5.5	**62.9**	**46.6**	6.3	1.4	**13.2**	**5.0**
Deciduous Broadleaf	Deciduous Forest	37.8	0.4	**79.1**	4.2	1.3	0.0	0.7	**7.4**	0.0
Evergreen Needleleaf	Evergreen Forest	1.0	NA	**5.1**	0.0	0.0	**12.9**	**16.2**	2.1	3.3
Tall Grass	Grassland, Herbaceous, Pasture, Hay	13.7	**61.3**	**7.6**	3.2	0.1	**20.7**	4.2	1.2	**3.8**
Crops	Cultivated Crops	28.3	**25.6**	0.5	**11.7**	0.2	**19.2**	0.6	0.0	0.0
Swamp (3.0 m)	Woody Wetlands	0.8	0.6	NA	**8.8**	0.4	**15.3**	**23.0**	0.6	0.9
Swamp (0.5 m)	Emergent Herbaceous Wetland	1.1	**4.0**	NA	1.3	0.0	1.7	**21.7**	**2.5**	0.4

[a]Items in bold indicate land use category was used in dry deposition calculations for that site.
[b]As defined by *Zhang et al.* [2003].
[c]As determined from the U.S. National Land Cover Database [*Homer et al.*, 2004].
[d]No dry deposition estimates were made for this site.

to identify processes such as input of plumes, photochemical formation/destruction, soil emission, deposition, and meteorology on trace gas concentrations [*Poulida et al.*, 1991; *Stamenkovic et al.*, 2007; *Selin et al.*, 2007]. Production of the plots averages the data and shows large, repeatable trends.

3.3. Wet and Dry Mercury Deposition

[19] Annual wet Hg deposition for the R-WI, R-ND, R-VA, U-WI, and C-SC sites was taken from records of co-located Mercury Deposition Network (MDN) sites (available at http://nadp.sws.uiuc.edu/MDN/) for the continuous 12-month period corresponding to the period of Hg speciation measurement (Table 1). For the C-AL, C-MA, and C-PR sites, wet Hg deposition samples from co-located samplers were collected weekly over the course of the corresponding mercury speciation measurement for each site. Samples for the 1-year period corresponding to data collection at those three sites were used in this study. Precipitation was collected in a pre-acidified PETG or glass bottle contained within an N-CON automated wet Hg deposition sampler. Samples for all sites were analyzed using dual amalgamation cold vapor atomic fluorescence. Wet Hg deposition data from the MDN network and samples from the C-PR site were analyzed for total Hg in the Frontier Geosciences laboratory (Seattle, Washington) while those collected at C-AL and C-MA were analyzed at the USGS Mercury Laboratory in Middleton, Wisconsin. Comparison of total Hg concentration in splits of precipitation samples demonstrates good analytical agreement between these two laboratories [*Weatherbee et al.*, 2006]. The U-IL site is not located adjacent to a wet Hg deposition sampler, so wet Hg deposition was estimated from the nearest MDN site (MO-46; ~175 km south of U-IL).

[20] Dry deposition of RGM and Hg-$PM_{2.5}$ was estimated using a numerical multiple resistance model (i.e., Big Leaf model). Similar models have been applied to estimate dry Hg deposition for previous studies [*Lyman et al.*, 2007; *Marsik et al.*, 2007]. Results from these studies indicate that when the canopy resistance term is ignored the resulting deposition velocity estimates for RGM compare well to results from surrogate surfaces [*Lyman et al.*, 2009]. Due to the large degree of uncertainty in adequately modeling the bi-directional flux of Hg^o and a lack of coarse Hg-P data for most sites, no attempt was made to model dry deposition of these species.

[21] Details of the dry deposition model, user guidance, computational procedures, parameter sensitivities, and references are extensively detailed by *Tate et al.* [2010]. The model is numerically similar to that of *Marsik et al.* [2007] but most notably differs by incorporating Land Use Categories (LUCs) of *Zhang et al.* [2003]. Briefly, RGM and Hg-$PM_{2.5}$ concentration data for each site were interpolated to estimate hourly average concentrations for each day of data. Hourly dry deposition flux of RGM and Hg-$PM_{2.5}$ was determined via

$$F_i = -V_d C_i, \tag{1}$$

where F_i is the flux of constituent i (either RGM or Hg-$PM_{2.5}$), V_d is the deposition velocity determined from the model using hourly average meteorological data corresponding to the period of measurement for C_i, the hourly average concentration of constituent i. For RGM, the deposition velocity is a function of the aerodynamic resistance (r_a), the quasi-laminar layer resistance (r_b), and the canopy resistance (r_c):

$$V_d = \frac{1}{r_a + r_b + r_c}. \tag{2}$$

The r_a and r_b terms are largely a function of inputs from site-specific meteorological parameters, while the r_c resistance depends on physiochemical properties of RGM and of the deposition surface (via LUCs). Likewise, hourly V_d values for Hg-$PM_{2.5}$ were calculated via

$$V_d = \frac{1}{r_a + r_b + r_a r_b v_s} + v_s, \tag{3}$$

where the impact of particle settling velocity (v_s) is included and the canopy resistance is replaced with a term dependant on r_a, r_b, and v_s.

[22] To characterize deposition to representative surfaces, land cover categories from the U.S. National Land Cover Database [*Homer et al.*, 2004] were determined within a 10 km radius for each site, converted to corresponding LUCs of *Zhang et al.* [2003], and are shown in Table 2. The purpose of choosing the 10 km radius was an attempt to give a "local" estimate of dry deposition in recognition that the environment that each site represents is composed of many vegetation/land cover types. To determine total flux for a site, the calculated deposition for each LUC was weighed by its portion of the 10 km surrounding each site.

[23] For sites where less than 1-year of RGM, Hg-$PM_{2.5}$, and meteorological data were available, dry deposition estimates for the period of measurement were linearly extrap-

Table 3. Summary of Seasonal Atmospheric Hg Speciation Concentration Data[a]

Site	Season	Hg^o (ng m^{-3})		RGM (pg m^{-3})		Hg-$PM_{2.5}$ (pg m^{-3})	
		$\bar{x} \pm \sigma$	Min.–Max.	$\bar{x} \pm \sigma$	Min.–Max.	$\bar{x} \pm \sigma$	Min.–Max.
R-WI	Spring	1.82 ± 0.24	1.22–3.55	11.2 ± 14.6	<dl–122	11.1 ± 7.7	0.56–44.7
	Summer	1.50 ± 0.33	0.45–6.48	3.8 ± 9.5	<dl–151	6.4 ± 3.8	<dl–26.3
	Fall	1.49 ± 0.23	0.27–3.26	2.9 ± 4.6	<dl–94.3	6.9 ± 5.9	<dl–72.2
	Winter	1.66 ± 0.19	0.92–3.08	2.8 ± 4.6	<dl–57.7	12.2 ± 11.8	<dl–205
R-ND	Spring	1.61 ± 0.22	0.99–5.13	2.0 ± 2.6	<dl–19.2	2.2 ± 2.4	<dl–11.9
R-VA	Summer	1.27 ± 0.31	<dl–3.63	1.8 ± 3.9	<dl–37.7	4.6 ± 3.9	<dl–19.4
U-IL	Fall	2.09 ± 1.49	1.00–64.1	11.6 ± 26.4	<dl–298	12.9 ± 12.7	<dl–104
	Winter	2.54 ± 5.35	0.05–324	63.3 ± 529	<dl–8,160	37.9 ± 492	<dl–11,600
U-WI	Spring	2.94 ± 1.56	1.66–17.9	12.2 ± 13.5	<dl–112	10.3 ± 22.2	<dl–507
	Summer	2.33 ± 0.76	1.29–7.65	13.8 ± 12.5	<dl–124	10.2 ± 13.8	<dl–333
	Fall	2.55 ± 0.97	1.45–12.8	10.1 ± 10.5	<dl–83.2	10.9 ± 8.7	<dl–95.3
	Winter	2.26 ± 0.98	1.73–24.7	4.1 ± 4.7	<dl–48.6	15.7 ± 13.3	<dl–171
C-AL	Spring	1.58 ± 0.23	0.29–4.65	4.7 ± 8.9	<dl–92.7	2.6 ± 3.3	<dl–32.1
	Summer	1.58 ± 0.26	0.97–16.4	2.5 ± 4.5	<dl–45.7	2.1 ± 1.7	<dl–20.3
	Winter	1.77 ± 0.23	0.97–6.18	4.2 ± 6.1	<dl–43.6	3.8 ± 4.3	<dl–44.7
C-SC	Spring	1.47 ± 0.22	0.25–2.61	3.8 ± 6.7	<dl–59.2	2.1 ± 2.0	<dl–13.9
	Summer	1.42 ± 0.25	0.45–6.09	2.8 ± 4.5	<dl–48.8	2.0 ± 4.2	<dl–84.7
	Fall	1.39 ± 0.26	0.28–3.80	3.8 ± 6.5	<dl–60.2	2.8 ± 3.1	<dl–18.8
	Winter	1.50 ± 0.24	0.31–7.55	2.9 ± 4.8	<dl–42.1	2.2 ± 2.3	<dl–21.1
C-MA	Spring	1.56 ± 0.23	0.48–3.81	3.0 ± 5.1	<dl–54.8	1.8 ± 2.2	<dl–19.9
	Summer	1.53 ± 0.19	1.10–6.74	2.4 ± 3.3	<dl–33.4	1.4 ± 1.1	<dl–10.7
	Fall	1.54 ± 0.33	0.96–3.29	2.0 ± 2.7	<dl–23.3	4.3 ± 6.1	<dl–38.3
	Winter	1.53 ± 0.20	0.93–2.80	3.2 ± 3.8	<dl–53.6	8.5 ± 6.3	<dl–37.1
C-PR	Spring	1.40 ± 0.14	1.04–3.72	1.5 ± 1.6	<dl–7.59	1.2 ± 1.4	<dl–13.4

[a]<dl = less than detection limit.

olated for a 1-year period. Meteorological data for the R-WI site were not of sufficient frequency to adequately calculate terms required in the model, so no estimates of dry deposition were made for the site.

4. Results and Discussion

4.1. Comparison of Mercury Speciation Data Between Sites

[24] Seasonal average Hg^o concentrations at the rural and coastal sites were typically 1.4–1.8 ng m^{-3} (Table 3). These values fall in the range of representative background tropospheric Hg^o concentrations in the Northern Hemisphere (1.3–1.8 ng m^{-3}) [*Valente et al.*, 2007] suggesting that, for the majority of data collected at these sites, Hg^o was primarily controlled by the global Hg pool rather than point Hg sources. However, seasonal mean Hg^o concentration at the high end, such as 1.82 ± 0.24 ng m^{-3} (mean ± standard deviation) measured at R-WI during the spring and 1.77 ± 0.23 ng m^{-3} at the C-AL site during winter, occurred during periods of significant input from regional Hg sources [*Rutter et al.*, 2008; *Engle et al.*, 2008a]. Conversely, a statistically lower mean Hg^o concentration at R-VA (summer only data) of 1.27 ± 0.31 ng m^{-3} may correspond to a period mixture of boundary layer and free tropospheric air masses [*Poulida et al.*, 1991]. *Banic et al.* [2003] observed lower concentrations of Hg^o in the free tropospheric air relative to boundary layer concentrations measured over background and metropolitan sites. Additionally, the speciation units report concentration in standard volumes of air; therefore, the actual Hg^o mean concentration at the 1,100 m elevation site was ~1.40 ng m^{-3}. In contrast to the majority of data from rural and coastal sites, elevated mean Hg^o concentrations were observed for all seasons at the two urban sites (2.09 ± 1.49 to 2.94 ± 1.56 ng m^{-3}). Maximum Hg^o concentrations for the urban sites (7.65 to 324 ng m^{-3}) also exceed corresponding data for the other sites often by more than an order of magnitude. These findings suggest that the two urban sites were impacted by year-round emissions from local and regional Hg sources.

[25] The seasonal mean RGM and Hg-$PM_{2.5}$ concentration data exhibited similar trends among sites to those found for Hg^o (Table 3). For both ionic Hg species, seasonal mean concentrations were <10 pg m^{-3} for all rural and coastal sites but concentrations as high as 63.3 ± 529 pg m^{-3} (RGM) and 37.9 ± 492 pg m^{-3} (Hg-$PM_{2.5}$) were measured at the urban sites. For both reactive species (RGM and Hg-$PM_{2.5}$) Kruskal Wallis and Dunn's multiple comparison tests indicate that concentrations of these species were higher at the U-IL and U-WI sites relative to the rural and coastal sites ($p<0.05$). For the U-WI site, the same tests indicate that Hg-$PM_{2.5}$ concentrations were significantly larger than other sites but, for RGM, concentrations were only statistically larger there than for the C–MA and C-SC sites. Despite relatively low seasonal mean values at the rural and coastal sites for most seasons, maximum RGM measurements (up to 150 pg m^{-3}) exceeded typical background concentrations (<15 pg m^{-3}) [*Valente et al.*, 2007] for nearly all sites and seasons (Table 3). Fine particulate Hg concentrations at the rural and coastal sites were typical for background sites (<25 pg m^{-3}) [*Valente et al.*, 2007] suggesting that, while complex processes may control Hg-$PM_{2.5}$ concentrations at these sites, these processes rarely lead to significant enrichment.

[26] Unlike Hg^o, which exhibits relatively low deposition rates (0.02–0.2 cm s^{-1}) [*Poissant et al.*, 2004; *Seigneur et al.*, 2004] and little diel variation in concentration (<15%) except near significant Hg sources, RGM concentrations tend to be more sporadic. Processes thought to produce significant sub-hourly variability in RGM concentrations include rapidly varying sinks (wet and dry deposition) and sources (impact

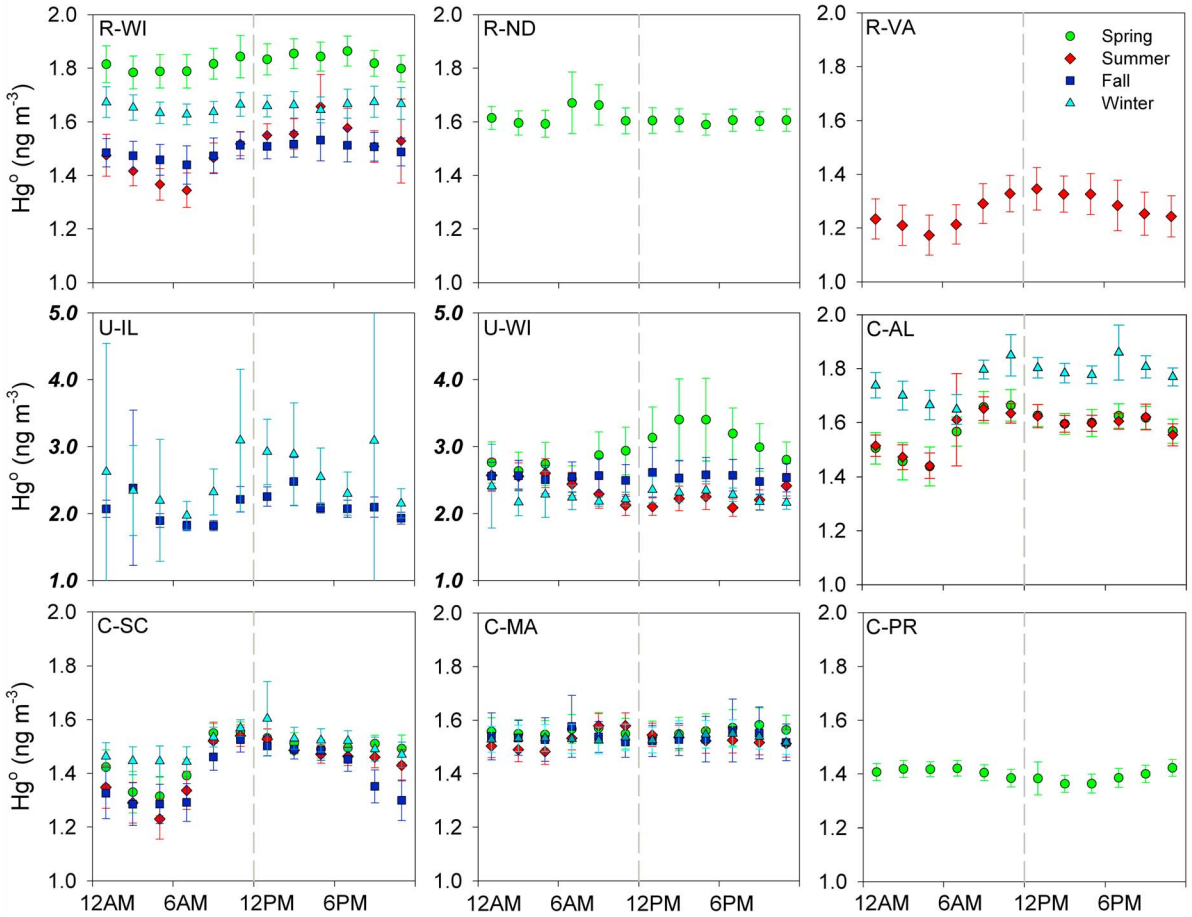

Figure 2. Diel bin plots showing $\bar{x} \pm \sigma$ of Hg^o concentrations over 2-h intervals throughout a 24-h day for each site and season. To minimize overlap, σ values were divided by 4. Figure 2 demonstrates significant differences in diel patterns and Hg^o concentrations between sites and seasons. Note change in y axis scale for data from the U-IL and U-WI sites. Noon is denoted with dashed vertical line.

from emissions sources, oxidation of Hg^o by photochemical species, volatilization of particulate Hg, and influx from RGM-rich regions of the free troposphere). Therefore, the variability of RGM concentrations at these sites may involve several factors, many of which will be further examined in this paper.

4.2. Diel Bin Plots of Elemental and Reactive Gaseous Mercury

[27] Using results from the diel bin plots, seasonal Hg^o concentration data were classified into 2 groups (Figure 2). The first group is characterized by < 0.1 ng m^{-3} variations in mean Hg^o concentrations between consecutive 2-h intervals, σ values < 2 ng m^{-3} (note that σ values are divided by 4 in Figures 2 and 3), and a range of concentrations typical for background sites (1.3–1.7 ng m^{-3}) [*Valente et al.*, 2007]. This group includes data for R-ND, R-VA, C-AL, C-SC, C-MA, C-PR and the fall, winter, and summer periods at R-WI. Despite diel variations in some of these data sets (discussed below), the relatively stable and background concentrations suggest that the global atmospheric Hg burden is the dominant source of Hg^o for these sites and seasons. However, maximum Hg^o concentrations at these sites often exceeded 1.7 ng m^{-3} (Table 3), indicating periodic impact from Hg point sources.

[28] The second group of data, including U-WI, U-IL, and the spring season for R-WI, are distinguished by seasonal mean Hg^o concentrations > 1.8 ng m^{-3}, erratic changes between consecutive 2-h averages, and σ values typically > 3 ng m^{-3}. These features indicate measurement of relatively frequent, short-lived Hg^o-rich pulses such as those intercepted downwind of local and regional point sources. This suggests that Hg^o concentrations and variability at these sites during these periods are primarily controlled by nearby Hg emission sources; although, inputs from the global Hg pool may also be important. This interpretation is consistent with previous conclusions for these data [*Manolopoulos et al.*, 2007a, 2007b; *Rutter et al.*, 2008].

[29] Subtle diel and seasonal Hg^o concentration variations were also observed (Figure 2). For example, mean Hg^o concentrations at the R-WI site were elevated in the spring (during maximum impact from regional point sources) [*Rutter et al.*, 2008] and winter relative to the summer and fall when uptake by biomass can decrease Hg^o concentrations [*Obrist*, 2007; *Obrist et al.*, 2008]. Mean Hg^o concentrations at the 1,100 m elevation R-VA site exhibited an early morning (~4 AM)

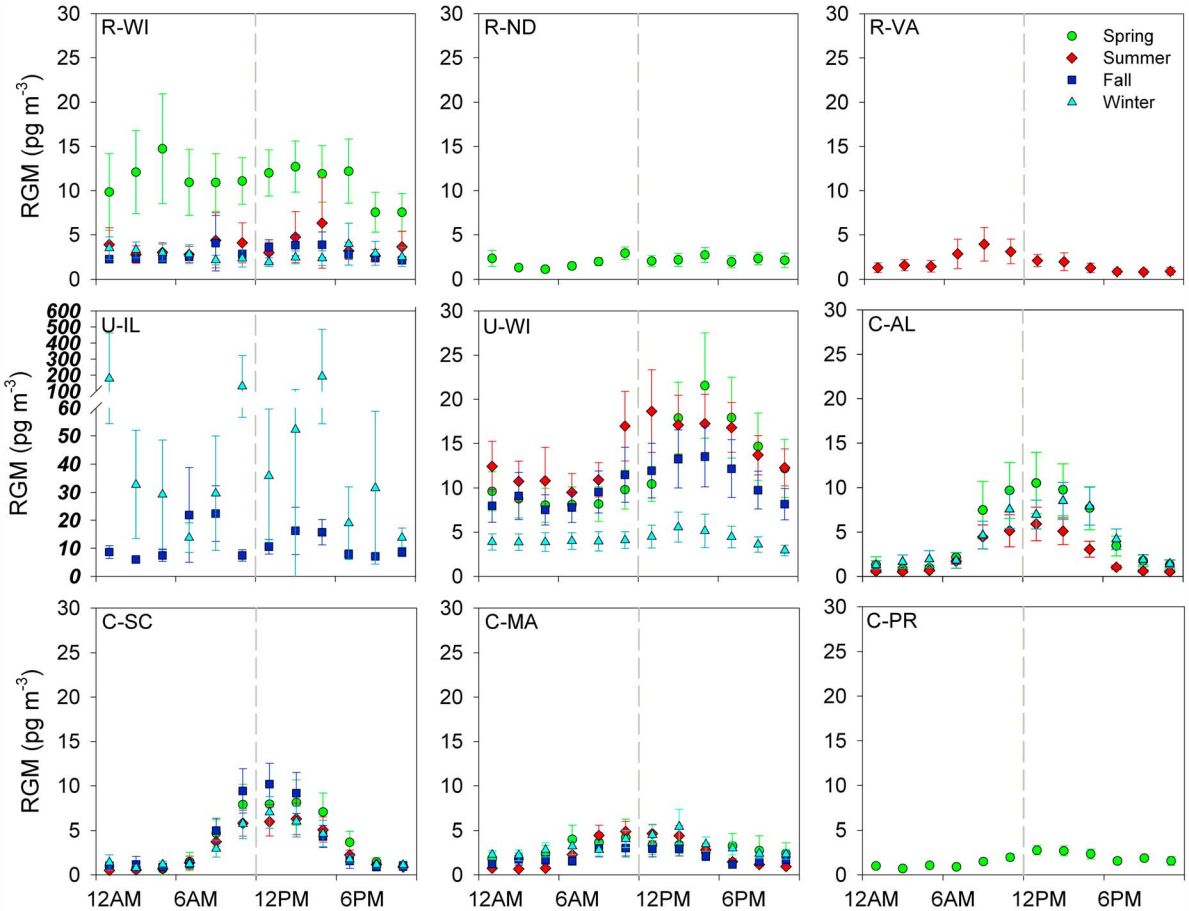

Figure 3. Diel bin plots showing $\bar{x} \pm \sigma$ of RGM similar to Figure 2. To minimize overlap, σ values were divided by 4. Note change in y axis scale for data from the U-IL site.

minimum and near noon maximum with periods of change in Hg^o concentration corresponding to transitions between free tropospheric and boundary layer air masses [*Poulida et al.*, 1991]. The noon-time maximum Hg^o concentrations likely resulted from nighttime and morning buildup of anthropogenic Hg emissions into the boundary layer in adjacent valleys that are transported up to the site in the late morning and early afternoon via heat-induced convection [*Obrist et al.*, 2008]. Data for all of the coastal sites and the R-WU site show an early morning (~6 AM) minimum, especially during the summer months. These early morning minimum Hg^o concentrations (i.e., Hg^o depressions) correspond with periods when the air temperature dipped down to or below the dew point (previously mentioned by *Rutter et al.* [2008]); an example is shown in Figure 4. A dew sample collected from an elevated polyethylene tarp at the C-SC site during one of these Hg^o depression events on 22 May 2007 contained 5.7 ng Hg L^{-1} (0.45 ng m^{-2}). While dew uptake may remove some Hg^o from the boundary layer, this simple estimate based on a single measurement would only remove <1% of the Hg^o from a > 100m thick boundary layer. Either the surrogate surface of the tarp behaved vastly different from natural surfaces or other processes, such as Hg removal by condensation in the Hg speciation units, caused disruption in Hg^o concentration/measurement during periods of extreme humidity [*Manolopoulos et al.*, 2007a]. Last, a small Hg^o concentration decrease (<0.1 ng m^{-3}) was observed from ~10 AM–6 PM at all of the coastal sites. Huber's method regression analysis of the Hg^o data confirms this statistically significant decrease ($p < 0.01$) for data from the C-AL, C-SC,

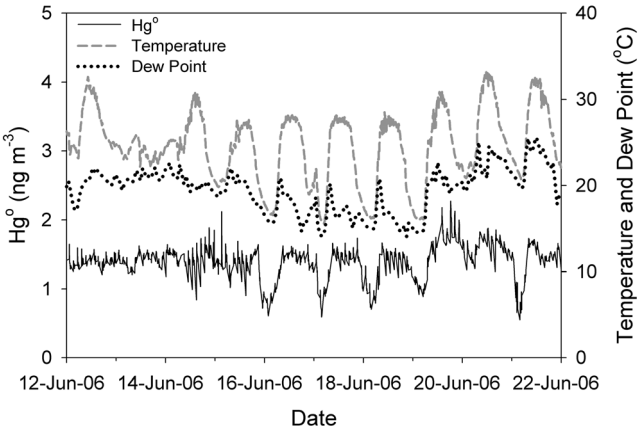

Figure 4. Time series of tropospheric Hg^o concentrations, air temperature, and dew point measured at the C-SC site from 12 to 22 June 2006. This plot demonstrates the correspondence of depressions in Hg^o concentration with periods when air temperature reaches the dew point.

and C-MA sites over the period of 11:00 AM–3:59 PM; the slope of regression line for the C-PR was not statistically significant from zero ($p = 0.79$). A small afternoon decrease in Hg^o could result either from a rapid loss of a small portion of Hg^o from the local boundary layer or from mixing with low-Hg air masses. We suggest that a small depletion in Hg^o is consistent with oxidation by photochemical compounds to RGM and/or Hg-P species, as discussed below.

[30] Diel bin plots of RGM data (Figure 3) were placed into three main categories: 1) those with mean RGM concentrations < 5 pg m^{-3} and little diel variability (e.g., R-ND and fall and winter at R-WI); 2) those showing mean RGM concentrations >10 pg RGM m^{-3} with significant, erratic diel variability and much larger σ values (e.g., spring data for R-WI, U-IL, U-WI); and 3) those exhibiting a consistent diel pattern of < 3 pg m^{-3} in the early morning increasing at ~6 AM to a daily maximum at noon, then decreasing back to < 3 pg m^{-3} by 6 PM and throughout the rest of the night (i.e., all coastal sites). The first category of data pattern is consistent with background RGM concentrations at non-impacted rural sites [*Kolker et al.*, 2008; *Rutter et al.*, 2008]. The second category of data includes sites where local and regional point sources are the primary sources of RGM [*Manolopoulos et al.*, 2007b; *Rutter et al.*, 2008]. The final category of data was found at the coastal sites and exhibits maximum noontime RGM concentrations with C-AL > C-SC > C-MA > C-PR, and RGM concentrations higher during the spring and fall and lower during the summer and winter seasons.

[31] Several possible mechanisms could account for the diel RGM concentration pattern exhibited at the coastal sites: 1) in situ oxidation of Hg^o by photochemical compounds to form RGM [*Chand et al.*, 2008; *Engle et al.*, 2008a]; 2) consistent, afternoon intrusions of RGM-enriched free tropospheric air masses into the boundary layer [*Swartzendruber et al.*, 2006; *Weiss-Penzias et al.*, 2009]; 3) meteorological conditions in which Hg emissions from point sources are emitted above the boundary layer during the night but daytime convection leads to mixing and exposure of the sites to elevated RGM concentrations [*Poissant et al.*, 2004]; and 4) sunlight-enhanced RGM emissions from natural surfaces such as Hg-enriched soils [*Gustin et al.*, 2006]. The last mechanism is unlikely to produce the measured RGM concentration pattern as evidenced by lack of a corresponding peak in Hg^o concentrations (Figure 2) and the presence of primarily low-Hg soils near these sites, which are unlikely to produce significant quantities of RGM through emission [*Engle et al.*, 2005; *Gustin et al.*, 2006]. While input of anthropogenic sources likely produces elevation of RGM concentrations during specific events, the diel RGM patterns observed at the coastal sites appear to discount mechanism 3 as the primary source of these patterns because: 1) co-contaminants show no corresponding peak with maximum RGM concentrations (e.g., Hg^o; Figure 2) or consistently peak several hours prior to maximum RGM concentrations (e.g., SO_2; see Figures S1–S4); 2) seasonal changes in diel patterns of the co-contaminants do not produce corresponding changes in diel RGM patterns (e.g., SO_2 data for the C-MA site; see Figure S2); and 3) the diel RGM trends for the coastal sites are distinctly different from those observed at point-source impacted rural and urban sites in that they exhibit early morning and late evening concentrations near zero, they display proportionally much lower standard deviation values (indicating less irregularity due to regular RGM-rich plumes), and they consistently manifest peak concentrations around noon, during maximum actinic flux (Figure 2). Intrusions of free tropospheric air (mechanism 2) are thought to be limited to continental deserts and high-elevation sites [*Selin et al.*, 2007], have shown to contain elevated RGM in relatively small pockets [*Sillman et al.*, 2007], and are typically associated with a decrease in CO concentration and humidity and an increase in O_3 concentration [*Swartzendruber et al.*, 2006; *Obrist et al.*, 2008; *Weiss-Penzias et al.*, 2009]. The latter two lines of evidence are ubiquitous during afternoon periods at most sites as a result of photochemical O_3 formation and daytime air temperature increase. Trace gas data for the coastal sites show daytime maximum concentrations of boundary layer–derived contaminants suggesting negligible mixing with supposedly SO_2 and CO depleted free tropospheric air masses during periods exhibiting the highest RGM concentrations (cf., Figure 3 and Figures S2 and S4). By elimination, we suggest that oxidation of Hg^o by a photochemical species controls RGM concentrations at the coastal sites; although, the other mechanisms may be important during specific, less frequent events. This interpretation is supported by a diel pattern where the highest concentrations correspond with maximum actinic flux (i.e., noon-time) and highly oxidizing conditions (Figure 3) and is consistent with a slight but statistically significant ($p < 0.01$) decrease in Hg^o concentrations during periods of maximum RGM concentrations at the coastal sites with the highest RGM concentrations (C-AL, C-SC, and C-MA). This finding also agrees with conclusions from previous coastal atmospheric Hg studies [*Malcolm et al.*, 2003; *Laurier and Mason*, 2007; *Chand et al.*, 2008; *Engle et al.*, 2008a].

[32] Ozone, OH·, and Br radicals have been cited as primary oxidants of Hg^o in the boundary layer [*Lindberg et al.*, 2002; *Pal and Ariya*, 2004; *Seigneur and Lohman*, 2008]. Relationships between these four coastal sites, which suggest RGM concentrations are controlled by oxidation via photochemical compounds, indicate that the highest RGM concentrations are associated with moist, warm environments with high concentrations of O_3 and moderate to low concentrations of NO_x, and likely VOCs (see Table S1). Although direct measurements are unavailable at the study sites, warm semi-polluted coastal environments are thought to generate high concentrations of OH· [*Thompson*, 1995]. Calculations for a site in Okinawa, Japan by *Chand et al.* [2008] suggest that, given concentrations of OH· typically found in coastal environments ($1–5 \times 10^6$ molecules cm^{-3}), reaction rates are fast enough to generate the elevated concentrations of RGM within a few hours. Other Hg^o oxidants such as O_3 [*Pal and Ariya*, 2004] and Br radicals [*Lindberg et al.*, 2002; *Calvert and Lindberg*, 2005; *Seigneur and Lohman*, 2008] are either thought to be too slow to generate significant concentrations of RGM in a <6 h duration or are lacking evidence of elevated RGM concentrations from marine-derived air masses (i.e., a Br radical dominated system; *Engle et al.* [2008a, 2008b]). However, arguments currently exist about the environmental viability of Hg^o oxidation to RGM species by OH· [*Pal and Ariya*, 2004; *Calvert and Lindberg*, 2005].

Table 4. Estimates of Annual Wet Deposition, Dry RGM Deposition, and Dry Hg-$PM_{2.5}$ Deposition for the Study Sites

Site	Period of Deposition Determination	Hg Precipitation Concentration (ng L^{-1})	Hg Wet Deposition (μg m^{-2} yr^{-1})	RGM Dry Deposition (μg m^{-2} yr^{-1})	Hg-$PM_{2.5}$ Dry Deposition (μg m^{-2} yr^{-1})	RGM + Hg-$PM_{2.5}$ Dry Deposition (μg m^{-2} yr^{-1})	Total Hg Deposition (μg m^{-2} yr^{-1})
R-WI	04 Oct 2003 – 04 Oct 2004	11.8	8.4	–	–	–	>8.4
R-ND	01 Jan 2004 – 12 Dec 2004	4.1	3.3	1.7	0.08	1.8	5.1
R-VA	01 Jan 2006 – 12 Dec 2006	6.8	9.0	1.4	0.14	1.5	10.5
U-WI	28 June 2004 – 6 June 2005	13.9	6.7	5.3	0.6	5.9	12.6
U-IL	01 Jan 2004 – 31 Dec 2004	9.7	11.0	51.8	1.5	53.3	64.3
C-SC	23 May 2006 – 22 May 2007	10.0	6.5	1.8	0.03	1.9	8.4
C-AL	12 April 2005 – 11 April 2006	8.8	10.9	2.2	0.05	2.2	13.1
C-MA	5 Feb 2008 – 3 Feb 2009	2.4	2.9	1.0	0.14	1.2	4.1
C-PR	1 Jan 2006 – 31 Dec 2006	10.6	29.5	0.5	0.02	0.5	30.0

4.3. Loading From Wet and Dry Deposition

[33] Modeled seasonal average V_d values for RGM and Hg-$PM_{2.5}$ from the dry deposition model range from 0.49 ± 0.42 to 5.01 ± 2.85 cm s^{-1} and 0.02 ± 0.01 to 0.37 ± 0.18 cm s^{-1}, respectively (results not shown), and are similar to those from previous studies (RGM = 0.4–2.1 cm s^{-1} and Hg-$PM_{2.5}$ = < 0.01–1.0 cm s^{-1}; *Lyman et al.* [2007]; *Marsik et al.* [2007]). These results suggest that dry Hg-$PM_{2.5}$ deposition is small relative to RGM deposition (Table 4). Dry deposition velocity calculations are highly dependent upon LUCs (Figure 5) suggesting that certain regions, especially urban areas, are predisposed to faster dry Hg deposition rates. The modeling results also indicate that meteorological parameters provide controls on dry deposition as evidenced by the significant variability observed among sites and seasons within the same LUC. In particular, sites with the fastest average wind velocities (see Table S1) typically exhibited faster dry deposition velocities for RGM (e.g., R-ND, U-WI, U-IL). This relationship exists because wind speed and friction velocity, which is a function of wind speed, are inversely proportional to the r_a and r_b resistance terms in equations (2) and (3) [*Tate et al.*, 2010].

[34] Thus, the fastest rates of dry RGM deposition were modeled for the U-IL (51.8 μg m^{-2} yr^{-1}) and U-WI (5.3 μg m^{-2} yr^{-1}) sites because they exhibited highly elevated RGM concentrations (up to >38,000 pg m^{-3}), displayed above average wind speeds, and were located in urban environments (Table 4). These results highlight the impact of local (<2 km) emission sources with short emission stacks (<50 m), which can generate highly elevated concentrations of reactive Hg species, on metropolitan areas [*Manolopoulos et al.*, 2007b]. Despite significantly different RGM and Hg-$PM_{2.5}$ concentrations between the other sites (Table 3), modeled dry deposition rates for all sites excluding C-PR are similar (0.5–2.2 μg m^{-2} yr^{-1}). The exceptionally low dry deposition at the C-PR site is driven by low RGM concentrations and slow wind velocity during the period of measurement.

[35] Estimates of total annual loading via dry deposition of RGM and Hg-$PM_{2.5}$ plus wet deposition range from 4.1 to 64.3 μg Hg m^{-2} yr^{-1} (Table 4 and Figure 6). Comparative analyses among sites should be done cautiously as the deposition estimates were calculated for different years. Comparison of wet versus dry Hg deposition shows that, with the exception of the U-IL site (wet deposition = 17%), wet deposition appears to be the primary mechanism (~65–98%) for transport of atmospheric Hg to surface environments. However, the dry deposition estimates lack information on Hg^o and coarse Hg-P deposition. For three different 7–8 day periods in 2006 and 2007 at the C-SC site, the coarse fraction (>2.5 μm) accounted for 66 ± 22% of total Hg-P concentrations and 30–46% of all Hg(II) dry deposition [*Engle et al.*, 2008b, also unpublished data, 2009]. Likewise, using Hg in leaf litter as an analog for net Hg^o deposition to New England forest canopies, *Miller et al.* [2005] found that Hg^o deposition is typically similar in magnitude to dry RGM deposition. Multiplying the dry deposition data by 2.5–3, to account for input from Hg^o and coarse Hg-P, the ratio of wet to dry Hg deposition at these sites is estimated at 0.4 to 2.4 with a median of 1.3, excluding U-IL (0.06) and C-PR (23). These crude estimates indicate that for all sites, except C-PR, dry deposition is a significant surface transport mechanism for Hg, which is on par with wet deposition.

[36] To assess the control of Hg sources on Hg deposition, total Hg emissions at distances of 10–50 km and 50–125 km (Table 1) were used to predict annual wet, dry (RGM + Hg-$PM_{2.5}$), and total Hg deposition (Table 4) using Huber's method robust regression. Sources within a 10 km radius

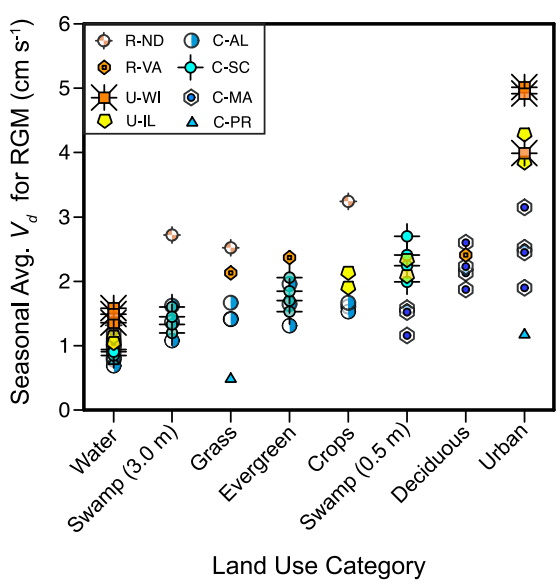

Figure 5. Variations in mean seasonal dry deposition velocity (V_d) of RGM between sites based on LUC. Figure 5 demonstrates the controlling role that canopy parameters (i.e., LUC) play in affecting dry RGM deposition velocities in modeling calculations.

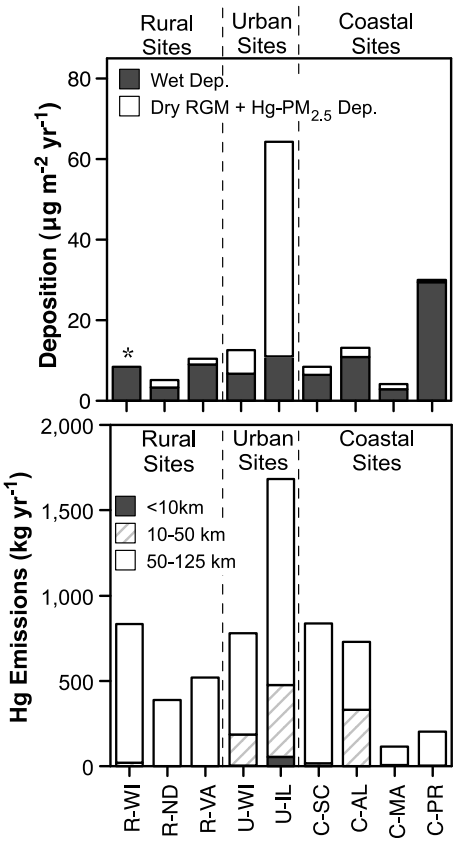

Figure 6. (top) Annual estimates of wet Hg deposition and dry deposition of RGM and Hg-$PM_{2.5}$. (bottom) Annual Hg emission estimates within <10 km, 10–50 km, and 50–125 km based on 2006 data from U.S. EPA Toxic Release Inventory (data available via http://www.epa.gov/triexplorer/) and the Canadian National Pollutant Release Inventory (data available via http://www.ec.gc.ca/inrp-npri/). Asterisk denotes no dry deposition estimates were made for the R-WI sites due to a lack of high-resolution meteorological data.

were not examined because they were quantifiable at only two study sites. This simple comparison is beneficial for determining the ability of Hg emission source magnitude to predict Hg deposition among the sites presented in this paper but lacks information of Hg speciation in the sources, spatial/meteorological relationships, and atmospheric chemistry. To better meet assumptions of normality, the 10–50 km Hg emissions, dry deposition, and total deposition values were transformed using square root and log base 10 functions. Regression results show no significant relationships ($p = 0.67$–0.95; $r^2 < 0.03$) between the magnitude of Hg emissions in the 10–50 km and 50–125 km categories with wet deposition loadings for these sites. These results highlight the demonstrated lack of spatial correlation between Hg emission sources and wet Hg deposition [*Miller et al.*, 2005; *Selin et al.*, 2007]. Conversely, dry and total Hg deposition loadings were significantly correlated with the magnitude of both 10–50 km and 50–100 km Hg emissions (adjusted $r^2 = 0.34$–0.78; p-value = 0.009–0.05). These results suggest that input from upwind emissions sources elevates concentrations of Hg species, leading to direct increases in dry deposition. However, if the two urban sites are removed from the regression analysis, the relationship between dry deposition and emissions decreases substantially. This finding highlights the importance of local emission sources with short dispersion stacks on dominating dry Hg deposition rates. While these simple regression models do not account for the complex chemical and meteorological relationships between Hg sources and sampling sites, they do suggest that close proximity with Hg emission sources does not appear to translate to high Hg deposition rates unless those sources include very short dispersion stacks, which can generate highly elevated concentrations of RGM and Hg-P.

5. Conclusions

[37] Comparison of atmospheric Hg speciation data between the nine rural, urban, and coastal sites examined in this paper allowed for separating local and regional processes from those operating on a near-continental to global scale. Use of the diel bin plots also identified complex atmospheric processes which impact atmospheric Hg cycling. For example, boundary layer-free tropospheric interactions, possible vegetative uptake of Hg^o, and impacts of plumes from Hg point sources were observed at a few of the sites during specific periods. Likewise, possible RGM formation via oxidation of Hg^o by photochemical species at all four coastal sites, input from the global Hg pool, and Hg^o depression during dew formation were observed at multiple sites suggesting these processes may play a significant role in continental or global Hg cycles. Comparison of meteorological and environmental conditions with the magnitude of the peak daily RGM concentrations indicates that Hg^o oxidation by photochemical compounds in coastal settings is exacerbated by warm, sunny, moist conditions with high concentrations of O_3 and moderate to low concentrations of NO_x, possibly by enhancing formation of OH·.

[38] Dry RGM and Hg-$PM_{2.5}$ deposition rates were elevated (5.3 and 51.8 $\mu g\ m^{-2}\ yr^{-1}$) at the two urban sites as a result of elevated concentrations of the two constituents and decreased calculated resistance to deposition resulting from high wind speed and coded parameters for urban environments. These high urban deposition rates created a significant correlation between Hg emission sources and dry deposition rates. Wet Hg deposition varied to a larger extent, but did not correlate well with the magnitude of area Hg emissions sources. These findings suggest that, for these sites, extrinsic factors may currently play a larger role in controlling wet Hg deposition than a few specific Hg point sources, but that the local point sources may be important for enhancing dry deposition. Accounting for dry deposition of Hg^o and coarse Hg-P, annual total Hg deposition at the sites ranged from 7.0 to >100 $\mu g\ m^{-2}$, indicating that dry deposition is an important pathway for Hg transport to surface environments for all sites except C-PR.

[39] Despite these advances, additional efforts are needed to understand the potential impacts from future Hg emissions regulations and to fill remaining data gaps. For example, ongoing research is currently developing better methods to quantify net Hg^o deposition and to examine the potential bioavailability of various atmospheric Hg species. Atmospheric modeling can also play an important role in examining how environmental variations between regions impact Hg cycling

processes and in forecasting changes in Hg behavior resulting from varying climactic and regulatory scenarios. It is hoped that this information will lead to a better understanding of the impacts of atmospheric Hg and to help develop better environmental regulations concerning Hg.

[40] **Acknowledgments.** Funding for this research was provided by the USGS Toxic Substances Hydrology Program, U.S. Department of Interior Landscapes Program, the USGS Mendenhall Postdoctoral Program, the USGS Energy Program, and by U.S. EPA STAR grant R829798. The authors are indebted to Virginia Garrison (USGS), Winston Luke (NOAA), and three anonymous journal reviewers for their comments and criticisms of the manuscript. Mark Olson and John DeWild provided significant support with instrumentation, multiple Tekran comparison studies, and data availability. Access and assistance were provided by personnel from the Weeks Bay National Estuarine Reserve, Cape Romain National Wildlife Refuge, Woods Hole Oceanographic Institute, U.S. Fish and Wildlife Service, Lostwood National Wildlife Refuge, Wisconsin Department of Natural Resources, U.S. National Park Service, and St. Louis-Midwest Particle Matter Supersite. Use of brand or trade names is for descriptive purposes and does not imply endorsement by the United States Government.

References

Banic, C., S. Beauchamp, R. Tordon, W. Schroeder, A. Steffen, K. Anlauf, and H. Wong (2003), Vertical distribution of gaseous elemental mercury in Canada, *J. Geophys. Res.*, *108*(D9), 4264, doi:10.1029/2002JD002116.

Calvert, J., and S. Lindberg (2005), Mechanisms of mercury removal by O_3 and OH in the atmosphere, *Atmos. Environ.*, *39*, 3355–3367, doi:10.1016/j.atmosenv.2005.01.055.

Chand, D., D. Jaffe, E. Prestbo, P. Swartzendruber, W. Hafner, P. Weiss-Penzias, S. Kato, A. Takami, S. Hatakeyama, and Y. Kajii (2008), Reactive and particulate mercury in the Asian marine boundary layer, *Atmos. Environ.*, *42*, 7988–7996, doi:10.1016/j.atmosenv.2008.06.048.

Edgerton, E., B. Hartsell, and J. Jansen (2006), Mercury speciation in coal-fired power plant plumes observed at three surface sites in the southeastern U.S., *Environ. Sci. Technol.*, *40*, 4563–4570, doi:10.1021/es0515607.

Engle, M. A., M. S. Gustin, S. E. Lindberg, A. W. Gertler, and P. A. Ariya (2005), The influence of ozone on atmospheric emissions of gaseous elemental mercury and reactive gaseous mercury from substrates, *Atmos. Environ.*, *39*, 7506–7517, doi:10.1016/j.atmosenv.2005.07.069.

Engle, M. A., M. T. Tate, D. P. Krabbenhoft, A. Kolker, M. L. Olson, E. S. Edgerton, J. F. DeWild, and A. K. McPherson (2008a), Characterization and cycling of atmospheric mercury along the central US Gulf Coast, *Appl. Geochem.*, *23*, 419–437, doi:10.1016/j.apgeochem.2007.12.024.

Engle, M. A., A. Kolker, D. P. Krabbenhoft, M. L. Olson, M. T. Tate, and C. Soneira (2008b), Mercury and other trace elements in coastal South Carolina aerosols, *Geochim. Cosmochim. Acta*, *72*, A244.

Fitzgerald, W., and C. Lamborg (2005), Geochemistry of mercury in the environment, in *Environmental Geochemistry, Treatise on Geochemistry*, vol. 9, edited by B. Sherwood-Lollar, pp. 107–148, Elsevier, New York.

Gustin, M. S., M. Engle, J. Ericksen, S. Lyman, J. Stamenkovic, and M. Xin (2006), Elemental Hg exchange between the atmosphere and low Hg containing substrates, *Appl. Geochem.*, *21*, 1913–1923, doi:10.1016/j.apgeochem.2006.08.007.

Helsel, D. R. (2005), *Nondetects and Data Analysis: Statistics for Censored Environmental Data*, 250 pp., John Wiley, Hoboken, N. J.

Homer, C., C. Huang, L. Yang, B. Wylie, and M. Coan (2004), Development of a 2001 national land-cover database for the United States, *Photogramm. Eng. Remote Sens.*, *70*, 829–840.

Kolker, A., M. A. Engle, W. H. Orem, J. E. Bunnell, H. E. Lerch, D. P. Krabbenhoft, M. L. Olson, and J. D. McCord (2008), Mercury, trace elements and organic constituents in atmospheric fine particulate matter, Shenandoah National Park, Virginia, USA: A combined approach to sampling and analysis, *Geostand. Geoanal. Res.*, *32*, 279–293, doi:10.1111/j.1751-908X.2008.00913.x.

Laurier, F., and R. Mason (2007), Mercury concentration and speciation in the coastal and open ocean boundary layer, *J. Geophys. Res.*, *112*, D06302, doi:10.1029/2006JD007320.

Lindberg, S. E., S. Brooks, C.-J. Lin, K. Scott, M. Landis, R. Stevens, M. Goodsite, and A. Richter (2002), Dynamic oxidation of gaseous mercury in the Artic troposphere at polar sunrise, *Environ. Sci. Technol.*, *36*, 1245–1256, doi:10.1021/es0111941.

Lyman, S., M. S. Gustin, E. M. Prestbo, and F. J. Marsik (2007), Estimation of dry deposition of atmospheric mercury in Nevada by direct and indirect methods, *Environ. Sci. Technol.*, *41*, 1970–1976, doi:10.1021/es062323m.

Lyman, S., M. S. Gustin, E. M. Prestbo, P. I. Kilner, E. Edgerton, and B. Hartsell (2009), Testing and application of surrogate surfaces for understanding potential gaseous oxidized mercury dry deposition, *Environ. Sci. Technol.*, *43*, 6235–6241, doi:10.1021/es901192e.

Malcolm, E. G., G. J. Keeler, and M. S. Landis (2003), The effects of the coastal environment on the atmospheric mercury cycle, *J. Geophys. Res.*, *108*(D12), 4357, doi:10.1029/2002JD003084.

Manolopoulos, H., J. J. Schauer, M. D. Purcell, T. M. Rudolph, M. L. Olson, B. Rodger, and D. P. Krabbenhoft (2007a), Local and regional factors affecting atmospheric mercury speciation at a remote location, *J. Environ. Eng. Sci.*, *6*(5), 491–501, doi:10.1139/S07-005.

Manolopoulos, H., D. Snyder, J. Schauer, J. Hill, J. Turner, M. Olson, and D. Krabbenhoft (2007b), Sources of speciated atmospheric mercury at a residential neighborhood impacted by industrial sources, *Environ. Sci. Technol.*, *41*, 5626–5633, doi:10.1021/es0700348.

Marsik, F. J., G. J. Keeler, and M. S. Landis (2007), The dry-deposition of speciated mercury to the Florida Everglades: Measurements and modeling, *Atmos. Environ.*, *41*, 136–149.

Mason, R., M. Abbott, R. A. Bodaly, O. R. Russell Jr., C. T. Driscoll, D. Evars, S. E. Lindberg, M. Murray, and E. B. Swain (2005), Monitoring the response to changing mercury deposition, *Environ. Sci. Technol.*, *39*, 14A–22A, doi:10.1021/es053155l.

Merritt, K. A., and A. Amirbahman (2009), Mercury methylation dynamics in estuarine and coastal marine environments: A critical review, *Earth Sci. Rev.*, *96*, 54–66, doi:10.1016/j.earscirev.2009.06.002.

Miller, E. K., A. Vanardsdale, G. J. Keeler, A. Chalmers, L. Poissant, N. C. Kamman, and R. Brulotte (2005), Estimation and mapping of wet and dry mercury deposition across northeastern North America, *Ecotoxicology*, *14*, 53–70, doi:10.1007/s10646-004-6259-9.

Obrist, D. (2007), Atmospheric mercury pollution due to losses of terrestrial carbon pools?, *Biogeochemistry*, *85*, 119–123, doi:10.1007/s10533-007-9108-0.

Obrist, D., A. Hallar, I. McCubbin, B. Stephens, and T. Rahn (2008), Atmospheric mercury concentrations at Storm Peak Laboratory in the Rocky Mountains: Evidence for long-range transport from Asia, boundary layer contributions, and plant mercury uptake, *Atmos. Environ.*, *42*, 7579–7589, doi:10.1016/j.atmosenv.2008.06.051.

Pal, B., and P. Ariya (2004), Gas-phase $HO^{\cdot}$-initiated reactions of elemental mercury: Kinetics, product studies, and atmospheric implications, *Environ. Sci. Technol.*, *38*, 5555–5566, doi:10.1021/es0494353.

Poissant, L., M. Pilote, X. Xu, H. Zhang, and C. Beauvais (2004), Atmospheric mercury speciation and deposition in the Bay St. Françios wetlands, *J. Geophys. Res.*, *109*, D11301, doi:10.1029/2003JD004364.

Poulida, O., R. Dickerson, B. Doddridge, J. Holland, R. Wardell, and J. Watkins (1991), Trace gas concentrations and meteorology in rural Virginia: 1. Ozone and carbon monoxide, *J. Geophys. Res.*, *96*(D12), 22,461–22,475, doi:10.1029/91JD02353.

Rutter, A. P., J. J. Schauer, G. C. Lough, D. C. Snyder, C. J. Kolb, S. V. Klooster, T. Rudolf, H. Manolopoulos, and M. L. Olson (2008), A comparison of speciated atmospheric mercury at an urban center and an upwind rural location, *J. Environ. Monit.*, *10*, 102–108, doi:10.1039/b710247j.

Sando, S. K., D. P. Krabbenhoft, K. M. Johnson, R. F. Lundgren, and D. G. Emerson (2007), Mercury and methylmercury in water and bottom sediments of wetlands at Lostwood National Wildlife Refuge, North Dakota, 2003–2004, *U.S. Geol. Surv. Sci. Invest. Rep. 2007–5219*, 66 pp.

Seigneur, C., and K. Lohman (2008), Effect of bromine chemistry on the atmospheric mercury cycle, *J. Geophys. Res.*, *113*, D23309, doi:10.1029/2008JD010262.

Seigneur, C., K. Vijayaraghavan, K. Lohman, P. Karamchandani, and C. Scott (2004), Global source attributions for mercury deposition in the United States, *Environ. Sci. Technol.*, *38*, 555–569, doi:10.1021/es034109t.

Selin, N., D. Jacob, R. Park, R. Yantosca, S. Strode, L. Jaegle, and D. Jaffe (2007), Chemical cycling and deposition of atmospheric mercury: Global constraints from observations, *J. Geophys. Res.*, *112*, D02308, doi:10.1029/2006JD007450.

Sillman, S., F. J. Marsik, K. I. Al-Wali, G. J. Keeler, and M. S. Landis (2007), Reactive mercury in the troposphere: Model formation and results for Florida, the northeastern United States, and the Atlantic Ocean, *J. Geophys. Res.*, *112*, D23305, doi:10.1029/2006JD008227.

Stamenkovic, J., S. Lyman, and M. Gustin (2007), Seasonal and diel variation of atmospheric mercury concentrations in the Reno (Nevada, USA) airshed, *Atmos. Environ.*, *41*, 6662–6672, doi:10.1016/j.atmosenv.2007.04.015.

Swartzendruber, P., D. A. Jaffe, E. M. Prestbo, J. E. Smith, P. Weiss-Penzias, N. E. Selin, D. J. Jacob, R. J. Park, S. Strode, and L. Jaegle (2006), Observations of reactive gaseous mercury at the Mt. Bachelor Observatory, *J. Geophys. Res.*, *111*, D24301, doi:10.1029/2006JD007415.

Tate, M. T., M. A. Engle, D. P. Krabbenhoft, E. B. Edgerton, and T. P. Meyers (2010), Numerical multiple resistance model to estimate gross dry deposition flux of atmospheric Hg species: Hg^o, RGM, Hg-PM_{fine}, Hg-PM_{coarse}, *U.S. Geol. Surv. Sci. Invest. Rep.*, in press.

Thompson, A. M. (1995), Measuring and modeling the tropospheric hydroxyl radical (OH), *J. Atmos. Sci.*, *52*, 3315–3327, doi:10.1175/1520-0469(1995) 052<3315:MAMTTH>2.0.CO;2.

Valente, R. J., C. Shea, K. L. Humes, and R. L. Tanner (2007), Atmospheric mercury in the Great Smoky Mountains compared to regional and global levels, *Atmos. Environ.*, *41*, 1861–1873, doi:10.1016/j.atmosenv.2006.10.054.

Weatherbee, G. A., N. E. Latysh, and S. M. Greene (2006), External quality-assurance results for the National Atmospheric Deposition Program/National Trends Network and Mercury Deposition Network, 2004, *U.S. Geol. Surv. Sci. Invest. Rep. 2006–5067*, 52 pp.

Weiss-Penzias, P., M. S. Gustin, and S. Lyman (2009), Observations of speciated atmospheric mercury at three sites in Nevada: Evidence for a free tropospheric source of reactive gaseous mercury, *J. Geophys. Res.*, *114*, D14302, doi:10.1029/2008JD011607.

Zhang, L., J. R. Brook, and R. Vet (2003), A revised parameterization for gaseous dry deposition in air-quality models, *Atmos. Chem. Phys.*, *3*, 2067–2082, doi:10.5194/acp-3-2067-2003.

M. H. Bothner, U.S. Geological Survey, 384 Woods Hole Rd., Woods Hole, MA 02543, USA.

M. A. Engle and A. Kolker, U.S. Geological Survey, 12201 Sunrise Valley Dr., Reston, VA 20192, USA. (engle@usgs.gov)

D. P. Krabbenhoft and M. T. Tate, U.S. Geological Survey, 8505 Research Way, Middleton, WI 53562, USA.

J. J. Schauer, Environmental Chemistry and Technology Program, University of Wisconsin-Madison, Madison, WI 53706, USA.

J. B. Shanley, U.S. Geological Survey, 87 State St., Montpelier, VT 05602, USA.